SUB-PIXEL UNPAVED ROADS DETECTION IN LANDSAT IMAGES

O. F. M. Gomes [a], R. Q. Feitosa [b], H. L. C. Coutinho [c]

[a] CETEM, Centre for Mineral Technology, Av. Ipê 900, 21941-590, Rio de Janeiro, Brazil – ogomes@cetem.gov.br
[a] Dept. of Materials Science and Metallurgy, Catholic University of Rio de Janeiro, Rua Marquês de S. Vicente, 225, Rio de Janeiro, 22453-900, Brazil
[b] Dept. of Electrical Engineering, Catholic University of Rio de Janeiro, Rua Marquês de S. Vicente, 225, Rio de Janeiro, 22453-900, Brazil – raul@ele.puc-rio.br
[b] Dept. of Computer Engineering, State University of Rio de Janeiro, Rua S. Francisco Xavier, 523, Rio de Janeiro 20550-900
[c] Embrapa-Soils, Rio de Janeiro, Brazil – heitor@cnps.embrapa.br

TS WG III/4 Automated Object Extraction

KEY WORDS: Road Detection, Object Recognition, Remote Sensing, Erosion Detection

ABSTRACT:

Unpaved roads are one of the most relevant causes of erosion process in rural regions. Locating unpaved roads in low-resolution satellite images is not a trivial task. Although they have the spectral response of bare soil, their spatial width is often far below the pixel size. Therefore, the pixels crossed by unpaved roads have a different spectral response over the scene depending on the surrounding pixels. In this work, a new method to detect sub-pixel unpaved roads is proposed. The method tries to emulate the human ability to detect such roads in spite of all appointed aspects, by searching for long, narrow and smooth line segments whose spectral response are closer to the bare soil than the surrounding pixels. The method performance is evaluated on segments of Landsat scenes (bands 3, 4 and 5) of the Alcinópolis County, located in the State of South Mato Grosso in Brazil.

1. INTRODUCTION

Large part of the Brazilian Midwest territory is highly susceptible to soil erosion events. These produce a range of negative environmental impacts, such as: formation of gullies; siltation of rivers, particularly those that drain to the Pantanal, the largest remaining wetlands of the world; land degradation; loss of terrestrial and aquatic biodiversity; water resources degradation; and social and economic burdens, mainly associated with the loss of agricultural land.

Non-sustainable land management practices are at the root of the worsening of erosion problems, being the most relevant the use of soil disruptive agricultural practices (disc harrowing, for eg.) and rural roads. Due to the growing impoverishment of the public sector in Brazil, associated with governmental commitments for payment of the foreign debt, most of the rural roads are still unpaved, and they are major inducers of soil erosion events, particularly in highly susceptible areas.

The ability to automatically detect rural roads in remotely sensed images would significantly enhance the efficiency of environmental managers in mapping areas highly susceptible to erosion events.

Road networks constitute a basic structure for the classification of land use / land cover from satellite images. In rural areas, unpaved narrow roads are quite frequent.

Most road detection methods proposed so far (see Duta 2000; Lin 2000; German 1996; Hui 2001; Mukherjee 1996; Rianto 1999; Rianto 2002) are applicable to high-resolution imagery where the road width is larger then the pixel size.

Locating unpaved roads in low to medium resolution satellite images is not a trivial task. Although they have the spectral response of bare soil, their spatial width is often far below the pixel size. Therefore, the pixels crossed by unpaved roads have a different spectral response over the scene depending on the surrounding pixels. In addition, the area covered by a scene may encompass more than one soil type, which increases the diversity of spectral appearance of unpaved roads over the image.

In this work, a new method to detect sub-pixel unpaved roads in multispectral low-resolution satellite images is proposed.

2. METHOD

Although pixels over unpaved narrow roads have spectral appearance dependent on the surroundings, a human being is often able to recognize them visually quite well. Figure 1 shows a sample segment of a LANDSAT image from the Taquari Watershed in Southwest Brazil. A RGB composition of bands 3, 4 and 5 is used. Rural roads in this area are less than 10 meter wide while pixel size in this case is 30 m to 30 m.

The image shows some roads crossing a pasture and a forest area. It is interesting to note that the roads across the forest have a similar spectral appearance as pasture. Therefore a simple spectral classification would assign the pixels of the roads crossing the forest to the class pasture. It is also worth noting

that even an untrained photo interpreter would be able in this example to locate the roads on the forest and on the pasture although they have quite different brightness in each case.

The method proposed in this paper exploits the following general assumptions regarding the characteristics of unpaved roads that are supposedly taken by a human observer into account to locate narrow unpaved roads on an image:

a) their color is more similar to the typical bare soil spectral appearance than are the pixels on both sides of the road,
b) they have medium to large length, and
c) direction changes smoothly along it.

The method proposes a set of attributes which express such characteristics. Once the attributes are selected the method consists of looking for one to two pixels wide lines on the image whose attributes values lie below appropriate thresholds.

The next sections introduce the attributes that capture the aforementioned characteristics. Later a detailed description of detection procedure is presented.

2.1 Unpaved Roads Attributes

Line length (characteristic b) can be easily measured. Attributes representing the relative similarity to the bare soil spectral response (characteristic a) and smoothness (characteristic c) are presented in the following.

Figure 1. An image segment from the Taquari Basin in Southwest Brazil.

2.1.1 Spectral Similarity to Bare Soil

Since the spectral response of a pixel crossed by an unpaved road depends on the neighboring pixels, thresholding segmentation cannot be employed. Thus, the detection procedure begins by modeling these pixels spectral response in relation to the surrounding. The model assumes that the response $\mathbf{p}_i$ of a pixel crossed by an unpaved road is the result of a linear combination of the response $\mathbf{p}_n$ of the land cover type of neighbor pixels and the response of bare soil $\mathbf{p}_b$, as stated below

$$\mathbf{p}_i = a \cdot \mathbf{p}_n + (1-a) \cdot \mathbf{p}_b + \boldsymbol{\varepsilon}_i \quad \text{for } 0 < a < 1 \tag{1}$$

where $\mathbf{p}_i$, $\mathbf{p}_n$ and $\mathbf{p}_b$ are vectors containing the reflectance at each spectral band of a pixel, its neighbor and bare soil, respectively, a is a scalar such that $0<a<1$ and $\boldsymbol{\varepsilon}_i$ is the model error.

$$\mathbf{p}_i - \mathbf{p}_b = a \cdot (\mathbf{p}_n - \mathbf{p}_b) + \boldsymbol{\varepsilon}_i \tag{2}$$

By defining $\mathbf{p}_{ib} = \mathbf{p}_i - \mathbf{p}_b$ and $\mathbf{p}_{nb} = \mathbf{p}_n - \mathbf{p}_b$ equation (2) takes the form

$$\mathbf{p}_{ib} = a \cdot \mathbf{p}_{nb} + \boldsymbol{\varepsilon}_i \tag{3}$$

Figure 2 shows the geometric interpretation of equations 1 to 3. The figure plane is defined by the points $\mathbf{p}_i$, $\mathbf{p}_n$ and $\mathbf{p}_b$ in the spectral space. Vectors $\mathbf{p}_{ib}$, $\mathbf{p}_{nb}$, $a\mathbf{p}_{nb}$ and $\boldsymbol{\varepsilon}_i$ are indicated close to their heads.

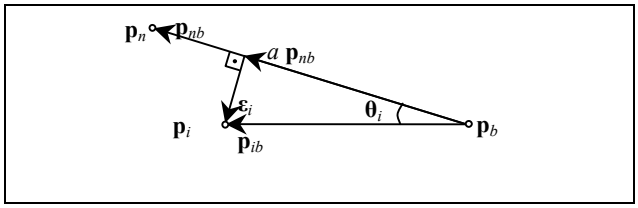

Figure 2. Geometric interpretation of the spectral response model for pixels crossed by unpaved roads.

The value of a for minimum error $|\boldsymbol{\varepsilon}_i|_{\min}$, can be obtained from Figure 1 or analytically as follows. From equation 3

$$\boldsymbol{\varepsilon}_i = \mathbf{p}_{ib} - a \cdot \mathbf{p}_{nb} \tag{4}$$

Therefore

$$|\boldsymbol{\varepsilon}_i|^2 = |\mathbf{p}_{ib}|^2 - 2 \cdot a \cdot |\mathbf{p}_{ib}| \cdot |\mathbf{p}_{nb}| \cdot \cos\theta_i + a^2 \cdot |\mathbf{p}_{nb}|^2 \tag{5}$$

where θ_i is the angle between $\mathbf{p}_{ib}$ and $\mathbf{p}_{nb}$. The derivative of the magnitude of the error is given by

$$\frac{\partial |\boldsymbol{\varepsilon}_i|^2}{\partial a} = -2 \cdot |\mathbf{p}_{ib}| \cdot |\mathbf{p}_{nb}| \cdot \cos\theta_i + 2 \cdot a \cdot |\mathbf{p}_{nb}|^2 \tag{6}$$

Making the derivative equal to zero and resolving for a it yields

$$\frac{\partial |\boldsymbol{\varepsilon}_i|^2}{\partial a} = 0 \Rightarrow a = \frac{|\mathbf{p}_{ib}|}{|\mathbf{p}_{nb}|} \cdot \cos\theta_i = \frac{\mathbf{p}_{ib} \cdot \mathbf{p}_{nb}}{|\mathbf{p}_{nb}|^2} \tag{7}$$

Replacing equation (7) in equation (5) results after some manipulation in:

$$|\boldsymbol{\varepsilon}_i|_{\min} = |\mathbf{p}_{ib}| \cdot \sin\theta_i \tag{8}$$

The absolute value of the error $|\boldsymbol{\varepsilon}_i|_{\min}$ is actually not a proper measure of how well a given pixel fits to the model. The magnitude of vector $\mathbf{p}_{ib}$ as well as $\mathbf{p}_{nb}$ for roads crossing pasture for example will be considerably lower than for roads in a forest region. That is because, pasture has already a spectral response much closer to bare soil than the forest. This can be observed in Figure 1. What actually counts is the error relative to the spectral response of the neighboring pixels. Dividing the error in equation (8) by the magnitude of vector $\mathbf{p}_{nb}$ results

$$|\boldsymbol{\varepsilon}_i|_n = \frac{|\mathbf{p}_{ib}|}{|\mathbf{p}_{nb}|} \cdot \sin\theta_i \tag{9}$$

This attribute does not depend on the spectral response of either sides of the road and expresses how well a pixel fits to the proposed model. So the smaller $|\boldsymbol{\varepsilon}_i|_n$ of a pixel, the greater its adherence to the model, and consequently the higher the possibility that it represents an unpaved narrow road.

2.1.2 Smoothness

A one pixel wide line is a sequence of $N+1$ pixels on coordinates (x_i,y_i) for $0 \le i \le N$ such that the pixel in (x_i,y_i) is adjacent to the pixel in (x_{i-1},y_{i-1}) for $0 < i \le N$. The angle φ_i determined by the tangent to the line at pixel x_i and the horizontal coordinate axis, can be approximated by

$$\varphi_i = \text{atan2}(y_i - y_{i-1}, x_i - x_{i-1}), \text{ for } 0 < i \le N \tag{10}$$

where atan2 is the four quadrant arctangent function. The rate of change of φ_i is the curvature of the line at pixel i (Sonka, 1999; Forsyth, 2003). The angle φ_i changes rapidly (slowly) on line segments with small (large) curvature. So the derivative of φ_i along the line relates to the curvature γ_i of a line at pixel i. This can be estimated by equation (11) below:

$$\gamma_i = \varphi_i - \varphi_{i-1}, \text{ for } 1 < i \le N \tag{11}$$

The average absolute curvature Γ of a line is given by equation (12) as the sum of absolute value of the curvature along all the line.

$$\Gamma = \frac{1}{N-2}\sum_{i=2}^{N}|\gamma_i| \tag{12}$$

Γ is high for smooth lines and low for sharp curves.

2.2 Detection Procedure

Once the measurements of the main road characteristic were introduced this section now presents the overall detection procedure. It consists of four sequential steps:

i) Preliminary road location
ii) Checking the spectral characteristics
iii) Checking the length limits
iv) Checking of the curvature limits

2.2.1 Preliminary Road Location

Analyzing all possible lines on the image is computationally impractical. Therefore a preliminary selection of possible unpaved roads is performed. This is done by measuring the normalized error given in equation (9) for each pixel.

Pixels for which the mixture parameter a does not fall in the interval [0, 1], as well as the pixels for which $|\mathbf{p}_{ib}| > |\mathbf{p}_{nb}|$ are immediately discarded. These conditions result from the model assumption that a pixel i on roads must be spectrally closer to bare soil than their neighbors.

A smoothed value of $\mathbf{p}_i$ is obtained by convolving each image band with a bank of oriented non-symmetric Gaussian filters with the general form given by equation (13) to (15)

$$H(x,y,\alpha) = k\exp\left[\frac{-1}{2}\left(\frac{x'^2}{\sigma_x^2}+\frac{y'^2}{\sigma_y^2}\right)\right] \tag{13}$$

$$x'^2 = x\sin(\alpha) + y\cos(\alpha) \tag{14}$$

$$y'^2 = x\cos(\alpha) - y\sin(\alpha) \tag{15}$$

where σ_x, σ_y are the standard deviation respectively along the direction x and y, α is the filter orientation and k is a constant assuring that the sum of all filter values equals 1. x' and y' represent coordinates after rotation α. For roads stretching along the y' direction σ_y/σ_x must be greater than one. Since the purpose is to detect roads narrower than the pixel size the value of σ_x must be selected in such a way that the Gaussian has values close to zero for a distance greater than 1 from the Gaussian center position. This assures that only pixels along the roads are considered in the evaluation of $\mathbf{p}_i$. In our experiments $\sigma_y=1$ and σ_x =1/3 were used.

Since the roads can stretch in different directions rotated versions of the Gaussian filters must be applied. Figure 3 shows the filters in four orientations as used in our experiments.

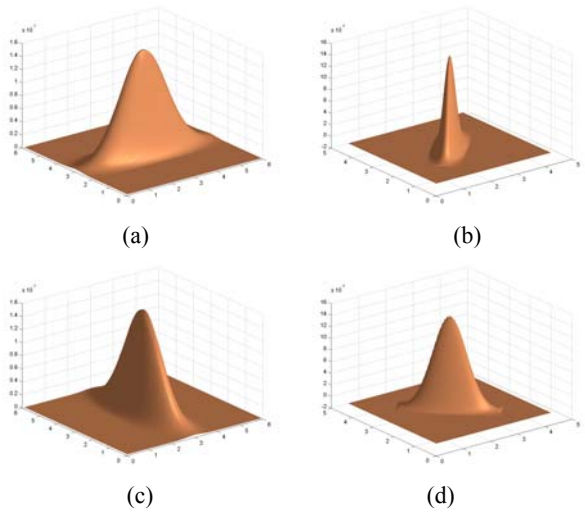

(a) (b) (c) (d)

Figure 3: Oriented Gaussian filter for (a) 0º orientation, (b) 45º orientation (c) 90º orientation and (d) 135º orientation.

The resulting matrix with the $\mathbf{p}_i$ values will be a blurred version of the input image. The spectral value representing the neighboring pixels $\mathbf{p}_n$ can also be obtained by convolving the image bands with the same oriented Gaussian filters, whereby the center of the filter is displaced around $6*\sigma_x$ pixels in the x' direction. Actually no further convolution to compute $\mathbf{p}_n$ will be necessary. The $\mathbf{p}_n$ matrix will be given by the $\mathbf{p}_i$ matrix of shifted by $6*\sigma_x$ pixels in the x' direction.

In fact, the spectral constraint must be met on both sides of the road. Therefore for each pixel two $\mathbf{p}_n$ values will be computed, one for either side of the road. Just the one corresponding to the lowest $|\boldsymbol{\varepsilon}_i|_n$ is kept for the next analysis steps.
The use of a set of oriented filters will produce as many values for $\mathbf{p}_i$ and $\mathbf{p}_n$, and consequently for $\mathbf{p}_{ib}$, $\mathbf{p}_{nb}$, and $|\boldsymbol{\varepsilon}_i|_n$, as the number of orientations α considered. The value corresponding to the lowest normalized error $|\boldsymbol{\varepsilon}_i|_n$ across all orientations is selected to represent that pixel in the following steps.

The spectral value for bare soil $\mathbf{p}_b$ must be provided by the user and is constant for a given image.

The two dimensional matrix **E** containing the normalized error $|\boldsymbol{\varepsilon}_i|_n$ of each pixel computed as explained is now used for the preliminary road detection.

In accordance to the assumption b) in section 2, a 3D representation of **E,** taking the intensities as the third dimension, is expected to reveal a sharp valley in the positions crossed by unpaved roads.

The minimum along these valleys are detected by suppressing any pixel response that is not lower than the two neighboring pixels on either side of it, considering the road direction given by the best α value. Figure 4 shows the result of this pre-selection procedure starting with the image of Figure 1.

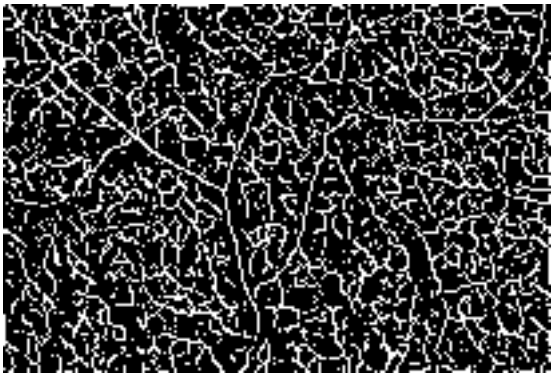

Figure 4. Result of preliminary road selection.

2.2.2 Checking the Spectral Characteristics

The three characteristics of the narrow unpaved roads mentioned in section 2 are then verified upon the pre-selected line candidates.

The tracking of the roads is initiated only on candidate pixels having an error $|\boldsymbol{\varepsilon}_i|_n$ inferior to a low threshold T_{sL}. Once started, the road is followed through the pixels whose error is now inferior to a high threshold T_{sH}. This is similar to the procedure applied by the Canny Edge Detector (Canny, 1986). Figure 5 shows the result of the road tracking for T_{sL}= 0.05 and T_{sH} = 0.25 applied to the result shown in Figure 4.

2.2.3 Checking the Length Limit

The length of all line segments remaining after the spectral checking is computed and compared to a length threshold T_l . Line segments whose length is inferior to T_l are discarded. The result of using T_l = 16 on the result of Figure 5 is shown in Figure 6.

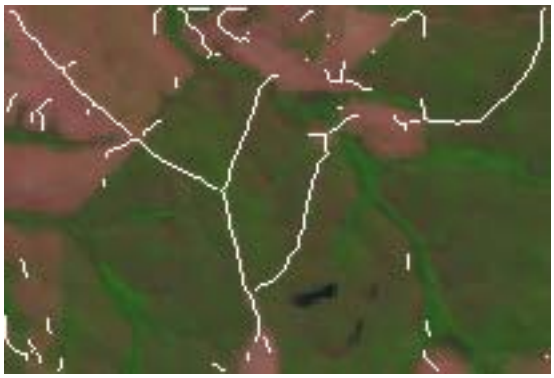

Figure 5. Result of road tracking.

Figure 6. Result after checking the length limit.

2.2.4 Checking the Curvature Limits

The average absolute curvature of each line segment that passed through the two previous verifications is computed and compared against a threshold T_c. The line segments of Figure 6 with an average absolute curvature Γ lower than 8 are shown in Figure 7.

Figure 7. Result after checking the curvature limit.

3. PERFORMANCE

A program implementing this method was written and applied to a set of multitemporal LANDSAT images from the Taquari Watershed, located in the Northeast of the State of Mato Grosso do Sul, in southwest of Brazil. Images were taken in August 1999, 2000 and 2001. The figures in this text come from a sample segment of these images. This area is suffering under

major environmental impacts mainly due to unplanned land occupation for cattle ranching and erosion is a major concern.

Since no ground truth data is available the performance evaluation was done visually by a photo interpreter. Actually this method does not intend to produce a final reliable result but instead, just to be an aid to the photo interpreter to locate narrow unpaved roads. It highlights the lines on the image having a high possibility of representing a road which will be later confirmed or disregarded during the visual edition.

The method requires the selection of four threshold values. Line length limits T_l and even the curvature limit T_c can be easily selected after some trials and errors. The two thresholds related to the spectral road characteristic T_{sL} and T_{sH} are not so intuitive and their selection is more cumbersome.

The sensibility of the method to the selection of threshold values was also tested. This affects mainly the detection of short lines but the long lines are equally detected for a variation of ± 5% around the optimal values. As a general evaluation the method proved to be an effective tool to improve the comfort and productivity of the photo interpretation in the task of detection narrow unpaved roads.

4. CONCLUSION

This works proposes a new method to detect sub-pixel unpaved roads on LANDSAT images. The method tries to emulate the reasoning of a human annalist by modelling road as narrow, long and smooth lines with a spectral response closer to that of bare soil than the neighbouring pixels. The method requires the manual selection of four parameters as well the spectral data of a typical bare soil.

Experiments on LANSAT images from the Midwest Brazil have shown that the method is a valuable aid to improve the productivity of the photo interpretation task as far as the detection of narrow unpaved roads is concerned.

Although the original motivation for this work was the erosion risk brought by unpaved roads, the proposed method has other potential practical applications. In the Amazon Region, for instance, there are a plenty of narrow rivers partially or even totally covered by the vegetation growing on the river banks, so that they become non-detectable to a conventional spectral classification. This method can be applied without any change to track the rivers through such areas, just by given the water spectral value instead of bare soil as input to the program.

Another potential application is gully detection, on images with similar LANDSAT resolution. Gullies are often narrow, and have in their initial formation a bare soil appearance which can be changed due to the vegetation growing over it. In this case short, instead of long segments, will be looked for.

These possibilities are to be investigated in the continuation of this research.

AKNOWLEDGMENT

We wish to thank PROBRAL (DAAD and CAPES funded Program) for their support to the ECOWATCH Project which this work is part of, and World Bank funded AGTEC project (Prodetab 093/01-98).

REFERENCES

Canny, J. 1986. A computational approach to edge detection, IEEE Trans. Pattern Anal. And Machine Intelligence, 8(6), pp. 679-698.

Duta, N. 2000. Road Detection in Panchromatic Spot Satellite Images, Proceedings of the 15th International Conference on Pattern Recognition, Vol. 4, pp. 308-311.

Lin, C., Wang, C.M., Chang, C. 2000. Application of Generalized Constrained Energy Minimization Approach to Urban Road Detection, Proceedings of the Geoscience and Remote Sensing Symposium - IGARSS '00, Vol. 5, pp. 2080-2082.

Forsyth, D.A., 2003, *Computer Vision – A Modern Approach*, Prentice Hall, pp. 429-434.

German, D., Jedynak B. 1996. An Active Testing Model for Tracking Roads in Satellite Images, IEEE Trans. Pattern Anal. And Machine Intelligence, 18(1), pp. 1-13.

Hui, A., Liew, S.C. Kwhoh, L.K. 2001. Extraction of Linear Features in Multiespectral Imagery, Geoscience and Remote Sensing Symposium - IGARSS '01, Vol. 5, pp. 2310-2312.

Mukherjee, A., Parui, S.K., Chaudhuri, D., Chaudhuri, B.B., Krishnan, R. 1996. An Efficient Algorithm for Detection of Road-Like Structures in Satellite Images. 13th International Conference on Pattern Recognition, Vol. 3, pp. 875-879.

Rianto, Y., Kondo, S, Kim, T. 1999. Detection of Roads from Satellite Image Using the Optimal Search, Proceedings. International Conference on Image Analysis and Processing, pp. 804-809.

Rianto, Y., 2002, Road network detection from SPOT satellite image using Hough transform and optimal search Asia-Pacific Conference on Circuits and Systems - APCCAS '02, Vol. pp. 177 – 180.

Sonka, M., Hlavac, V., Boyle, R., 1999, *Image Processing Analysis and Machine Vision*, PWS Publishing, pp. 237, 244.